

Mass measurements of neutron-rich indium isotopes for r -process studies

C. Izzo ^{1,*} J. Bergmann,² K. A. Dietrich,^{1,3} E. Dunling,^{1,4} D. Fusco,⁵ A. Jacobs,^{1,6} B. Kootte,^{1,7} G. Kriepkó-Koncz,^{2,†} Y. Lan,^{1,6} E. Leistenschneider,^{1,6} E. M. Lykiardopoulou,^{1,6} I. Mukul,¹ S. F. Paul,^{1,3} M. P. Reiter,^{1,2,8} J. L. Tracy, Jr.,¹ C. Andreoiu,⁹ T. Brunner,^{1,10} T. Dickel,^{2,11} J. Dilling,^{1,6} I. Dillmann,^{1,12} G. Gwinner,⁷ D. Lascar,^{1,13} K. G. Leach,¹⁴ W. R. Plaß,^{2,11} C. Scheidenberger,^{2,11} M. E. Wieser,¹⁵ and A. A. Kwiatkowski^{1,12}

¹TRIUMF, 4004 Wesbrook Mall, Vancouver, British Columbia, Canada V6T 2A3

²II. Physikalisches Institut, Justus-Liebig-Universität, 35392 Gießen, Germany

³Ruprecht-Karls-Universität Heidelberg, D-69117 Heidelberg, Germany

⁴Department of Physics, University of York, York YO10 5DD, England, United Kingdom

⁵Department of Physics and Astronomy, University of Waterloo, Waterloo, Ontario, Canada N2L 3G1

⁶Department of Physics and Astronomy, University of British Columbia, Vancouver, British Columbia, Canada V6T 1Z1

⁷Department of Physics and Astronomy, University of Manitoba, Winnipeg, Manitoba, Canada R3T 2N2

⁸School of Physics and Astronomy, University of Edinburgh, Peter Guthrie Tait Road, Edinburgh EH9 3FD, Scotland, United Kingdom

⁹Department of Chemistry, Simon Fraser University, Burnaby, British Columbia, Canada V5A 1S6

¹⁰Physics Department, McGill University, Montréal, Québec, Canada H3A 2T8

¹¹GSI Helmholtzzentrum für Schwerionenforschung GmbH, Planckstraße 1, 64291 Darmstadt, Germany

¹²Department of Physics and Astronomy, University of Victoria, Victoria, British Columbia, Canada V8P 5C2

¹³Center for Fundamental Physics, Northwestern University, Evanston, Illinois 60208, USA

¹⁴Department of Physics, Colorado School of Mines, Golden, Colorado 80401, USA

¹⁵Department of Physics and Astronomy, University of Calgary, Calgary, Alberta, Canada T2N 1N4



(Received 24 November 2020; accepted 8 February 2021; published 25 February 2021)

A new series of neutron-rich indium mass measurements is reported from the TITAN multiple-reflection time-of-flight mass spectrometer (MR-TOF-MS). These mass measurements cover $^{125-134}\text{In}$ ($N = 76-85$) and include ground states as well as isomeric states. The masses of nuclei in this region are known to be of great importance for accurately modeling r -process nucleosynthesis, and the significance of the reported neutron-rich indium masses is discussed in this context. Results are compared with earlier experimental data where available as well as theoretical mass models. The measurements reported here include the first mass measurements of $^{133,134}\text{In}$, as well as the first direct mass measurement of ^{132}In . The masses of $^{125-131}\text{In}$ in ground states and several isomers were previously measured to higher precision by Penning trap mass spectrometry, which also resolved some low-lying isomers that could not be resolved in this work. The earlier Penning trap measurements serve as excellent cross-checks for the MR-TOF-MS measurements, and in some cases the MR-TOF-MS measurements improve the literature uncertainties of higher-lying isomer masses and excitation energies. A new isomeric state for ^{128}In , recently reported for the first time by the JYFLTRAP group, is also confirmed by the TITAN MR-TOF-MS, with a measured excitation energy of 1813(17) keV.

DOI: [10.1103/PhysRevC.103.025811](https://doi.org/10.1103/PhysRevC.103.025811)

I. INTRODUCTION

The astrophysical rapid neutron-capture process (r process) plays a crucial role in explaining the origin of the chemical elements in the universe, accounting for approximately half of the production of elements heavier than iron [1]. A complete understanding of the r process has so far been limited due to the need for reliable experimental nuclear data for neutron-rich nuclei far from the valley of stability. Experimental nuclear physics continues to illuminate

this understanding through measurements of nuclear properties such as masses, β -decay properties, and neutron capture rates, which serve as both direct inputs into astrophysical calculations and benchmarks for theoretical models extending to very neutron-rich nuclei beyond the reach of current experimental methods.

Nuclear masses or, more precisely, mass differences play a particularly important role in r -process calculations, appearing in the form of β -decay Q values $Q_{\beta^-} = M(Z, N) - M(Z + 1, N - 1)$ and neutron separation energies $S_n(Z, N) = M(Z, N - 1) - M(Z, N) + M_n$, where $M(Z, N)$ is the atomic mass of the atom with Z protons and N neutrons and M_n is the mass of a free neutron. A recent sensitivity study by Mumpower *et al.* [2] identified the nuclei which have the most significant impact on final r -process abundances

*cizzo@triumf.ca

†Part of doctoral thesis, Justus-Liebig-Universität Gießen, in preparation.

in multiple astrophysical conditions. In all scenarios, the masses of nuclei in the region of the $N = 82$, $Z = 50$ double shell closure, particularly those with $Z \lesssim 50$, were found to be of great importance for calculating r -process abundances. This is due to the bottleneck in the r -process reaction flow known to occur near the double shell closure, which leads to the second r -process abundance peak around mass $A = 130$ [1].

As of the most recent atomic mass evaluation, the AME2016 [3], masses of many neutron-rich indium ($Z = 49$) isotopes in this region were not well known. Only the masses of $^{129-131}\text{In}$ had been measured directly, with $^{129,131}\text{In}$ measured using the JYFLTRAP Penning trap [4] and $^{130,131}\text{In}$ measured using the Canadian Penning Trap (CPT) [5]. In the CPT measurements, an unknown mixture of ground and isomeric states was observed, and the reported ^{131}In mass differed from the JYFLTRAP value by 149 keV. Furthermore, these Penning trap measurements of indium isotopes and other masses in that region frequently found deviations of more than 100 keV from masses determined indirectly via β end-point measurements, which suggested a systematic error in the β end-point derived masses (see, for example, the discussion in Refs. [5,6]), additionally demonstrating the need for accurate, direct mass measurements.

More recently, a series of high-precision Penning trap mass measurements was carried out at TRIUMF's Ion Trap for Atomic and Nuclear Science (TITAN) [7], measuring the masses of indium ground states and several long-lived ($t_{1/2} > 100$ ms) isomers from $A = 125$ to 130 [8]. JYFLTRAP has also recently reported new Penning trap mass measurements of $^{128,130}\text{In}$ [9], including the observation of a new isomeric state for ^{128}In and resolving a low-lying isomer for ^{130}In that was not resolved in the previous CPT or TITAN measurements.

The work reported here is a continuation of the campaign to measure the masses of neutron-rich indium isotopes in this region, now taking advantage of the addition of a multiple-reflection time-of-flight mass spectrometer (MR-TOF-MS) [10,11] to the suite of ion traps available at TITAN. The high sensitivity of the TITAN MR-TOF-MS and the ability to cope with extreme signal-to-background ratios allowed these measurements to proceed several mass units further away from stability, now measuring out as far as ^{134}In . This marks the first mass measurements of $^{133,134}\text{In}$ and the first direct mass measurement of ^{132}In .

In total, ten mass units were covered from $A = 125$ to 134 so that the MR-TOF-MS measurements could be benchmarked against the Penning trap measurements previously published from TITAN, JYFLTRAP, and CPT [4,5,8]. A precision of $\frac{\delta m}{m} \approx 3 \times 10^{-7}$ (corresponding to an uncertainty ≈ 40 keV for the measured mass range) was achieved in most cases, and the MR-TOF-MS reached three neutron-rich indium isotopes further from stability than any Penning trap measurement to date. Furthermore, the MR-TOF-MS measurements included several high-lying isomeric states that were not seen in the narrower mass range of the TITAN Penning trap measurements. In some cases the MR-TOF-MS measurements of the excitation energies of these high-lying isomers have smaller uncertainties than the current litera-

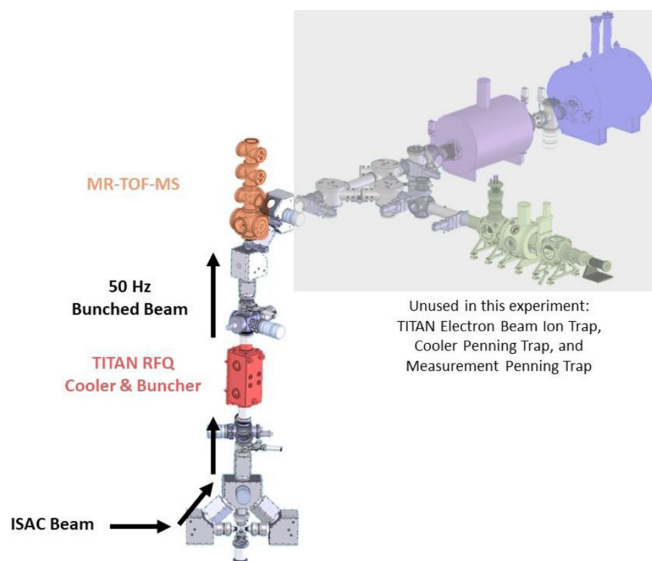


FIG. 1. Schematic overview of the TITAN experimental devices used for this work.

ture values obtained from spectroscopy measurements. These measurements and their impact for the astrophysical r process are discussed in the following sections.

II. EXPERIMENT

A schematic overview of the TITAN facility is presented in Fig. 1. The neutron-rich indium isotopes measured in this work were produced at the Isotope Separator and Accelerator (ISAC) facility [12] at TRIUMF. A uranium carbide target was bombarded with a $10\text{-}\mu\text{A}$ proton beam at an energy of 480 MeV, and the extracted indium isotopes were selectively ionized using the ion-guide laser ion source (IG-LIS) [13]. The IG-LIS suppresses surface ions with an electrostatic potential barrier and extracts the ions created by laser ionization beyond the barrier through a radio-frequency quadrupole (RFQ) to guide them toward the extraction. The desired mass unit was selected using the ISAC mass separator [14], and the radioactive beam was then delivered to the TITAN facility [7], where it was cooled and bunched in a linear RFQ [15] filled with helium buffer gas. Ion bunches $\approx 1 \mu\text{s}$ in length were then sent to the MR-TOF-MS at a rate of 50 Hz.

The TITAN MR-TOF-MS is based on the design of the system used by the Giessen-GSI collaboration [16,17] and uses the time-of-flight method [18,19] to determine the masses of singly charged ions of interest from the relative time of flight compared to some reference ions of well-known mass. The MR-TOF-MS consists of a helium-filled rf transport system and injection trap, an electrostatic time-of-flight mass analyzer, and a MagneTOF detector [11]. Cooled ion bunches from the TITAN RFQ undergo additional cooling in the rf transport and injection sections and then enter the mass analyzer section, where they are reflected between two electrostatic mirrors [20] to achieve a long path length for time-of-flight separation in a relatively compact space. A mass-range selector [17,21] is used in the analyzer to

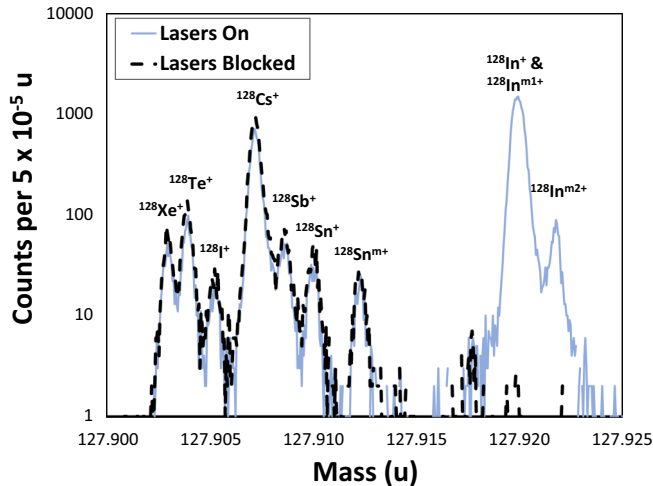


FIG. 2. Mass spectrum for $A = 128$ with lasers on (tuned on indium, solid line) and one laser transition blocked (dashed line). When the laser is blocked, the indium peaks disappear, providing peak identification verification.

deflect any particle outside the desired mass window, ensuring all ions detected have undergone the same number of reflections. The ions are then sent to the MagneTOF detector, which records their flight time. The dynamical time focus shift method [22] is used to adjust the time focus of the ion bunches to the MagneTOF. For this experiment, ions were reflected through 300–360 turns (one turn includes a reflection from each of the two electrostatic mirrors), corresponding to ≈ 8 ms of flight time, in order to achieve a typical mass resolving power of $\approx 230\,000$.

At each mass unit, data were collected with the resonant ionization laser from the IG-LIS on as well as blocked in order to verify the identity of the indium peak or peaks in the mass spectrum. As seen in Fig. 2, when the laser was blocked, the ionized indium was nearly eliminated from the beam, while the rate of other species remained constant.

The overall rate of the radioactive beam sent to TITAN was limited to keep an average of approximately one detected ion per cycle in the MR-TOF-MS in order to eliminate systematic uncertainties arising from ion-ion interactions inside the mass analyzer. For $A = 131$ – 134 , the rate of indium was several orders of magnitude lower than the rates of contaminant species, especially stable or near-stable cesium, and thus the mass-selective retrapping technique [23] was required to suppress this background. This technique was first used in an experiment to study neutron-deficient ytterbium isotopes [24]. Ions passed through the mass analyzer for a number of turns to achieve sufficient separation and then were dynamically recaptured in the rf injection trap, with the recapture timing chosen to accept the indium ions of interest while rejecting the background. The ions were then released again into the mass analyzer for normal measurement. In the TITAN system, this technique can typically suppress the background by a factor of $\approx 10^4$ while keeping ions of interest with an efficiency of approximately 50%. As a result, a much higher overall beam rate (and thus a higher rate of the neutron-rich indium ions of

interest) could be sent to TITAN while still maintaining only approximately one ion per cycle in the analyzer following the mass-selective retrapping.

This superior background handling ability, in combination with the sensitivity of the MR-TOF-MS, makes it an ideal tool for measurements far from stability. The most exotic isotope measured in this work, ^{134}In , was detected at the MR-TOF-MS at an average rate of only ≈ 0.01 ions per second. This rate was sufficient to bring the statistical uncertainty of the mass measurement below the limiting systematic uncertainty within a few hours of measurement.

III. ANALYSIS

The time-of-flight spectra were converted to mass spectra using the calibration function

$$m/q = c(t - t_0)^2 \quad (1)$$

where c and t_0 are calibration parameters, m/q is the mass-to-charge ratio, and t is the time of flight. The parameter t_0 represents a small timing offset which arises from signal propagation and electronic delays and was measured to be $t_0 = 164(2)$ ns immediately prior to the experiment from a single-turn spectrum using stable $^{85,87}\text{Rb}$ and ^{133}Cs from offline ion sources. The parameter c was determined for each mass unit from an isobaric reference ion of well-known mass that arrived with the radioactive beam from the ISAC target. A time-dependent calibration [25,26] was applied to each spectrum to correct for temperature drifts and power-supply instabilities.

The masses of the ions of interest were determined by fitting the mass spectrum peaks for the calibrants and the ions of interest using the hyperexponentially modified Gaussian (hyper-EMG) fitting routine developed for MR-TOF-MS analysis [27]. The hyper-EMG fit uses a Gaussian center convoluted with a variable number of asymmetric exponential tails. This procedure has been shown to produce accurate mass values even in cases where overlapping peaks are fit [26]. The presence of unresolved isomers can often be deduced from a broadening of the peak shape. The ability to detect and accurately fit such overlapping peaks heavily depends on case-specific factors such as statistics, the mass difference between the overlapping peaks, and their relative areas. It also requires a well-defined peak shape, established by parameters of the hyper-EMG fit from a calibration peak which is measured under the same conditions; has higher statistics than the ion of interest; and does not overlap with any other peak. A full description of the analysis procedure, including the treatment of overlapping peaks, is presented in Ref. [26].

A systematic uncertainty of $\delta m/m_{\text{sys}} = 3 \times 10^{-7}$ [21] is included in the reported mass uncertainties. This systematic uncertainty was previously determined as an upper limit for the TITAN MR-TOF-MS based on accuracy measurements with a stable-isotope beam, and is dominated by the effects of a nonideal electrical switching for ion ejection from the mass analyzer, causing calibrants and ions of interest to potentially experience slightly different electrical fields on ejection from the analyzer.

TABLE I. Mass excesses for $^{125-134}\text{In}$ ground states and isomers measured in this work, given in keV. Measurements used singly charged ions for all indium and reference species. Previous literature values are presented as well: ground-state mass excesses are from AME2016 [3] and isomer mass excesses are taken from NUBASE2016 [28]. Mass excesses from the TITAN Penning trap measurements (Babcock2018) [8] and the recent JYFLTRAP measurements (Nesterenko2020) [9] are listed for comparison as well. Listed half-lives and spin/parity assignments are from ENSDF [29–37], except for $^{128}\text{In}^{m2}$, which comes from Ref. [9].

Isotope	$T_{1/2}$	J^π	Ref.	Mass excess (keV)			
				This work	AME/NUBASE2016	Babcock2018	Nesterenko2020
$^{125}\text{In}^a$	2.36 s	9/2 ⁺	^{125}Cs	−80 511(110)	−80 477(27)	−80 412.4(15)	
$^{126}\text{In}^a$	1.53 s	3 ⁽⁺⁾	$^{63}\text{Cu}_2$	−77 785(44)	−77 773(27)	−77 809.5(41)	
^{127}In	1.09 s	(9/2 ⁺)	^{127}Cs	−76 873(37)	−76 896(21)	−76 876(11)	
$^{127}\text{In}^{m1}$	3.67 s	(1/2 [−])	^{127}Cs	−76 469(37)	−76 487(21)	−76 487(15)	
$^{127}\text{In}^{m2}$	1.04 s	(21/2 [−])	^{127}Cs	−75 126(36)	−75 030(60)	−75 179(48)	
^{128}In	0.84 s	(3 ⁺)	^{128}Cs	−74 183(38)	−74 150(150)	−74 170.5(97)	−74 190.0(14)
$^{128}\text{In}^{m1}$	0.72 s	(8 [−])	^{128}Cs	−73 924(44)	−74 060(30)	−73 908.8(91)	−73 904.9(21)
$^{128}\text{In}^{m2}$	≥ 0.3 s	(16 ⁺)	^{128}Cs	−72 370(39)			−72 392.4(15)
^{129}In	611 ms	(9/2 ⁺)	^{129}Cs	−72 846(37)	−72 837.7(27)	−72 836.4(61)	
$^{129}\text{In}^{m1}$	1.23 s	(1/2 [−])	^{129}Cs	−72 399(37)	−72 380(3)	−72 392(14)	
$^{129}\text{In}^{m2a}$	0.67 s	(23/2 [−])	^{129}Cs	−71 196(89)	−71 180(50)		
$^{130}\text{In}^a$	0.29 s	1 ^(−)	^{130}Xe	−69 893(43)	−69 880(40)	−69 862(20)	−69 909.2(75)
$^{130}\text{In}^{m2}$	0.54 s	(5 ⁺)	^{130}Xe	−69 523(38)	−69 480(50)	−69 503(28)	−69 524.1(33)
^{131}In	0.28 s	(9/2 ⁺)	$^{12}\text{C}^1\text{H}_3\ ^{116}\text{Sn}$	−68 051(40)	−68 025.0(27)		
$^{131}\text{In}^{m1}$	0.35 s	(1/2 [−])	$^{12}\text{C}^1\text{H}_3\ ^{116}\text{Sn}$	−67 675(39)	−67 660(7)		
$^{131}\text{In}^{m2}$	0.32 s	(21/2 ⁺)	$^{12}\text{C}^1\text{H}_3\ ^{116}\text{Sn}$	−64 280(38)	−64 280(90)		
^{132}In	0.200 s	(7 [−])	^{132}Cs	−62 395(38)	−62 410(60)		
^{133}In	165 ms	(9/2 ⁺)	$^{12}\text{C}^1\text{H}_3\ ^{118}\text{Sn}$	−57 678(41)	−57 460(200) ^b		
$^{133}\text{In}^m$	180 ms	(1/2 [−])	$^{12}\text{C}^1\text{H}_3\ ^{118}\text{Sn}$	−57 036(69)	−57 130(200) ^b		
^{134}In	140 ms	(4 [−] to 7 [−])	$^{12}\text{C}^1\text{H}_3\ ^{119}\text{Sn}$	−51 855(44)	−51 660(300) ^b		

^aIndicates cases where ME and uncertainty were adjusted to account for unresolved isomers (see text for details).

^bIndicates extrapolated literature values.

An additional uncertainty was introduced in four cases where a known isomer with a half-life longer than 1 ms was unresolved from the ground state or another isomer by the MR-TOF-MS, and only one peak containing an unknown ratio of the two states could be fit. In these cases, the standard AME protocol [3] was followed, in which the atomic mass is determined by

$$M_0 = M_{\text{exp}} - \frac{1}{2}E_1, \quad (2)$$

and the uncertainty is given by

$$\sigma_0^2 = \sigma_{\text{exp}}^2 + \left(\frac{1}{2}\sigma_1\right)^2 + \sigma^2, \quad (3)$$

where $M_0 \pm \sigma_0$ is the ground-state mass and uncertainty, $E_1 \pm \sigma_1$ is the isomer excitation energy and uncertainty, $M_{\text{exp}} \pm \sigma_{\text{exp}}$ is the measured mass and uncertainty of the peak containing the unknown mixture of ground state and isomer, and $\sigma^2 = \frac{1}{12}E_1^2$. The four cases where this procedure was required were ^{125}In , ^{126}In , $^{129}\text{In}^{m2}$, and ^{130}In . In the case of $^{129}\text{In}^{m2}$, $^{129}\text{In}^{m2}$ was well resolved from the ground state and first isomeric state, but could not be fit separately from $^{129}\text{In}^{m3}$. In this case, $^{129}\text{In}^{m2}$ was treated as M_0 in Eq. (3), and $E_1 = 281.0(2)$ keV (from ENSDF [33,37]) was used for the energy difference between the two unresolved isomers. The isomer excitation energy for ^{125}In was taken from the current ENSDF evaluation [29,37], while the isomer excitation energies used for the evaluation of ^{126}In and ^{130}In were taken from the

recent TITAN [8] and JYFLTRAP [9] Penning trap measurements, respectively, as these had smaller uncertainties than the ENSDF values.

In cases where ground and isomeric states were both observed and could be fit independently, isomer excitation energies were determined from the mass difference between ground and isomeric states. In these cases, the systematic uncertainty from the nonideal electrical switching for ion ejection from the mass analyzer was significantly reduced, as the ground-state and isomeric state peaks are expected to experience similar extraction fields. Based on offline tests performed prior to this experiment, an estimated systematic uncertainty of 5–6 keV (depending on the ions' total flight time for a given measurement) due to non-ideal ejection was included in the reported isomer excitation uncertainties.

IV. RESULTS

The measured ground-state and isomeric state mass excesses are presented in Table I, and isomer excitation energies are presented in Table II. Figure 3 compares isomer excitation energies from this work with values from ENSDF [29–37] and from the recent TITAN [8] and JYFLTRAP [9] Penning trap measurements. Individual cases are discussed below. Isomer naming ($m1$, $m2$, ...) throughout this work only counts isomers with half-lives $t_{1/2} > 1$ ms, meaning those that survived

TABLE II. Excitation energies for the neutron-rich indium isomers measured in this work. Previous literature values from ENSDF [29–37] are presented as well as the TITAN Penning trap measurements (Babcock2018) [8] and the recent JYFLTRAP measurements (Nesterenko2020) [9]. In cases where the isomer excitation energies from ENSDF differ from those reported in NUBASE2016, the NUBASE values [28] are also listed in brackets. Listed half-lives and spin/parity assignments are from ENSDF, except for $^{128}\text{In}^{m2}$, which comes from Ref. [9].

Isotope	$T_{1/2}$	J^π	Isomer excitation energy (keV)			
			This work	ENSDF [NUBASE2016]	Babcock2018	Nesterenko2020
$^{127}\text{In}^{m1}$	3.67 s	(1/2 ⁻)	406(12)	408.9(3)	390(18)	
$^{127}\text{In}^{m2}$	1.04 s	(21/2 ⁻)	1744(9)	1863(58) [1870(60)]	1697(49)	
$^{128}\text{In}^{m1}$	0.72 s	(8 ⁻)	259(28)	340(60) [80(160)]	262(13)	285.1(25)
$^{128}\text{In}^{m2}$	≥ 0.3 s	(16 ⁺)	1813(17)			1797.6(20)
$^{129}\text{In}^{m1}$	1.23 s	(1/2 ⁻)	447(13)	459(5) [458(4)]	444(15)	
$^{129}\text{In}^{m2a}$	0.67 s	(23/2 ⁻)	1649(82)	1630(56) [1660(50)]		
$^{130}\text{In}^{m2}$	0.54 s	(5 ⁺)	370(25)	400(60)	359(34)	385.5(50)
$^{131}\text{In}^{m1}$	0.35 s	(1/2 ⁻)	375(18)	302(32) [365(8)]		
$^{131}\text{In}^{m2}$	0.32 s	(21/2 ⁺)	3771(15)	3764(88) [3750(90)]		
$^{133}\text{In}^m$	180 ms	(1/2 ⁻)	642(60)	330(40) ^b		

^aIndicates cases where excitation energy and uncertainty were adjusted to account for unresolved isomers (see text for details).

^bIndicates extrapolated literature values.

long enough to be observed in the TITAN MR-TOF-MS. The current ENSDF value for the half-life and spin/parity of each species is listed in Tables I and II for additional clarity.

A. ^{125}In

The masses of ^{125}In and $^{125}\text{In}^{m1}$ were previously measured by the TITAN Penning trap with an uncertainty of 1.5 and 13 keV, respectively [8]. $^{125}\text{In}^{m1}$, with an excitation energy of 360.12(9) keV [38,39], was not resolved from the ground state by the TITAN MR-TOF-MS. The ground-state mass of ^{125}In reported here was therefore determined according to the AME protocol [3] for unresolved isomers present at an unknown ratio, as discussed in the previous section. This procedure assumes an equal ratio of ground and isomeric states in the beam delivered from ISAC, and then inflates the uncertainty accordingly. The 98.6-keV difference between the TITAN MR-TOF-MS mass and the TITAN Penning trap mass [8] is likely an indication that more ground state was present than isomer. The ^{125}In ground-state mass has the largest uncertainty of any mass reported in this work (110 keV) due to this unresolved 360.12-keV isomer. $^{125}\text{In}^{m2}$ ($t_{1/2} = 5.0$ ms [40]) was also observed in this work, lying in the tail of the much larger peak including ^{125}In and $^{125}\text{In}^{m1}$. Further analysis is required for an accurate mass determination of this isomer, and will be presented separately in a future paper.

B. ^{126}In

Similar to the ^{125}In case, $^{126}\text{In}^m$ (102-keV excitation energy) could not be resolved from the ground state. The ground-state mass and uncertainty were adjusted as described previously. Both the ^{126}In ground state and isomer were previously measured to high precision with the TITAN Penning trap [8]. The reported MR-TOF-MS ground-state mass agrees with the Penning trap value.

C. ^{127}In

^{127}In , $^{127}\text{In}^{m1}$, and $^{127}\text{In}^{m2}$ were all sufficiently separated by the MR-TOF-MS that each peak could be fit separately. The ground-state mass agrees well with the Penning trap value. The $^{127}\text{In}^{m1}$ excitation energy has been determined to an uncertainty of 0.3 keV in the ENSDF evaluation [31,37], based on a fit to observed γ rays following the decay of ^{127}Cd [41]. It was also measured previously by the TITAN Penning trap [8] with an 18-keV uncertainty. The MR-TOF-MS measurement reported here has a 12-keV uncertainty and agrees more closely with the ENSDF value than the Penning trap value, though it agrees with both within one standard deviation.

The $^{127}\text{In}^{m2}$ excitation energy was previously measured to an uncertainty of 58 keV based on Q_{β^-} measurements [42]. The TITAN Penning trap measurement [8] found a 166-keV deviation from the Q_{β^-} measurement, with a 49-keV error bar. The MR-TOF-MS measurement reported here confirms the deviation found by the Penning trap and reduces the uncertainty to 9 keV.

D. ^{128}In

It is interesting to compare the ^{128}In and $^{128}\text{In}^{m1}$ masses measured by the TITAN [8] and JYFLTRAP [9] Penning traps and the TITAN MR-TOF-MS. The two Penning trap masses agree well for $^{128}\text{In}^{m1}$ but differ by 20(10) keV for the ^{128}In ground state, resulting in a difference of 23(13) keV for the $^{128}\text{In}^{m1}$ excitation energy. The MR-TOF-MS ground-state mass agrees more closely with the JYFLTRAP value, however the $^{128}\text{In}^{m1}$ mass differs from both Penning trap values by >15 keV, and as a result the $^{128}\text{In}^{m1}$ excitation energy reported in this work agrees more closely with the TITAN Penning trap value than the JYFLTRAP value. It may be worth noting that both the TITAN Penning trap and MR-TOF-MS measurements rely on two-state fits of overlapping ground and isomeric states, while the JYFLTRAP measurement fully

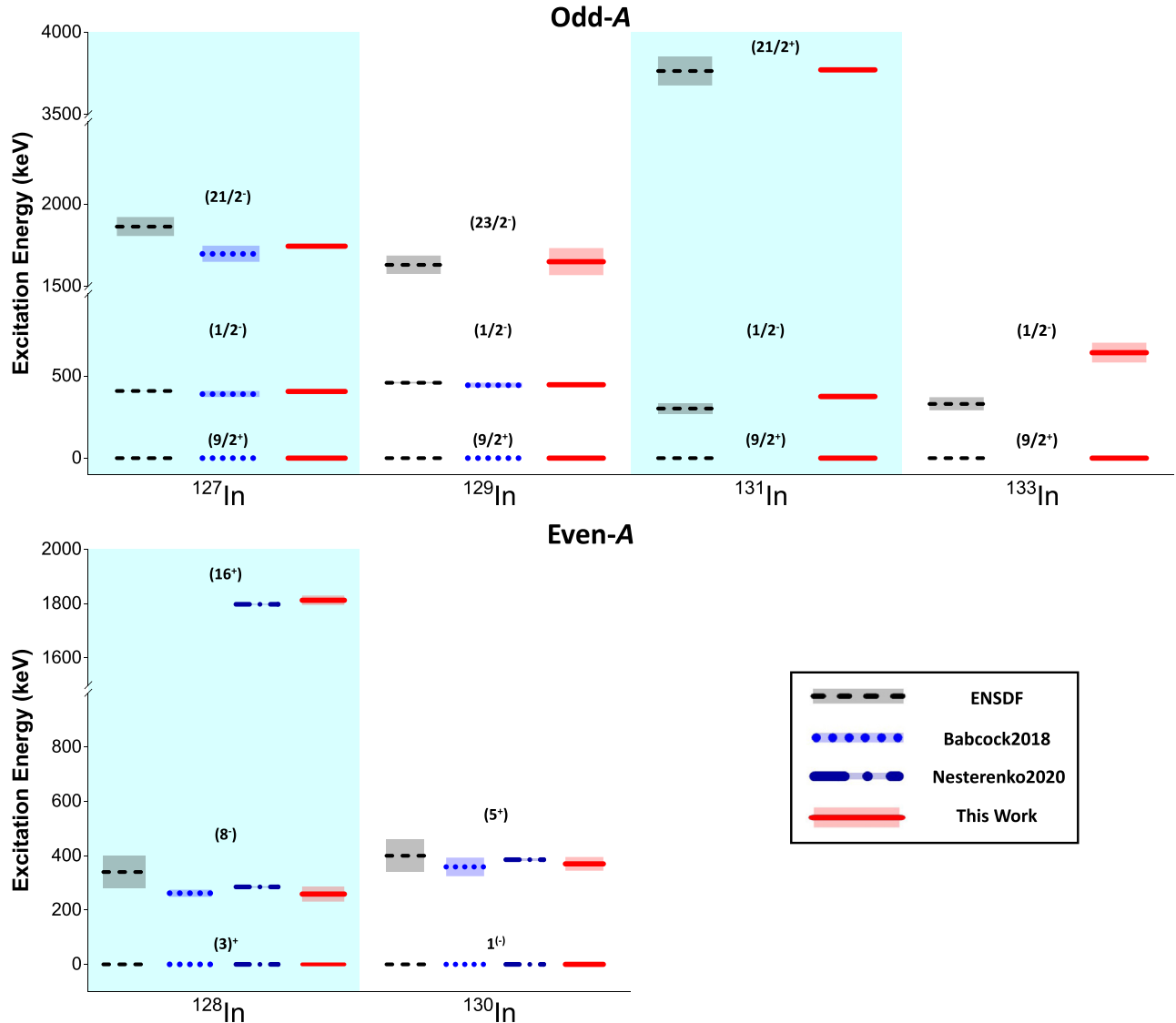


FIG. 3. Isomer excitation energies measured in this work, plotted in comparison to those reported in ENSDF [37] and the recent Penning trap measurements from TITAN [8] and JYFLTRAP [9]. Bands indicate the uncertainty. Note that isomeric states not measured in this work, including those with $t_{1/2} < 1$ ms and those that could not be fit separately from the ground state, are not included here. The utility of the MR-TOF-MS as a tool for measuring isomer excitation energies is clear, improving literature uncertainties in several cases and observing a number of isomers not measured previously by the TITAN Penning trap due to the MR-TOF-MS's sensitivity, background handling abilities, and non-scanning measurement technique.

separated the two states, resulting in a smaller reported uncertainty for the JYFLTRAP measurements.

A new ^{128}In isomer, notated as $^{128}\text{In}^{m2}$ in Table I, was also observed with an excitation energy of 1813(17) keV. As shown in Fig. 2, this peak essentially disappeared along with the other ^{128}In peak when the indium resonant ionization laser was blocked, confirming that the unknown peak was indium related. The new isomer was very recently studied and reported by the JYFLTRAP Penning trap facility [9]. The JYFLTRAP measurement found an excitation energy of 1797.6(20) keV, which agrees with the value reported here within the uncertainty, and suggested a half-life greater than 0.3 s for $^{128}\text{In}^{m2}$. A (16^+) spin/parity assignment was also suggested by the JYFLTRAP work, based on post-trap

spectroscopy studies and comparison with shell-model calculations. In the previous TITAN Penning trap measurement of ^{128}In , this isomer would not have been observed if present as the scanned frequency range did not extend far enough away from the ground state.

E. ^{129}In

The ground-state mass of ^{129}In measured by the MR-TOF-MS agrees with the values measured previously by the JYFLTRAP and TITAN Penning traps [4,8]. The excitation energy of $^{129}\text{In}^{m1}$ was also measured previously by both Penning traps, with the JYFLTRAP measurement published separately from the ground-state measurement [43]. The

reported excitation energies were 459(5) and 444(15) keV, respectively. The $^{129}\text{In}^{m1}$ excitation energy measured by the TITAN MR-TOF-MS is 447(13) keV, in agreement with both Penning trap measurements.

The excitation energies of $^{129}\text{In}^{m2}$ and $^{129}\text{In}^{m3}$ have not been measured by a Penning trap. The excitation energy of $^{129}\text{In}^{m2}$ was previously determined to be 1630(56) keV based on its Q_{β^-} difference from the ground state [42]. In that same work, the isomer $^{129}\text{In}^{m3}$ was proposed based on an observed 281-keV γ transition with a 110-ms half-life, which was suggested to be an $E3$ transition from $^{129}\text{In}^{m3}$ to $^{129}\text{In}^{m2}$. This would result in a 1911(56)-keV excitation energy for $^{129}\text{In}^{m3}$. These two isomeric states could not be resolved by the MR-TOF-MS, so a single peak fit was used to fit the two unresolved states and the reported mass of $^{129}\text{In}^{m2a}$ was adjusted as described previously.

F. ^{130}In

^{130}In has a low-lying isomer with an excitation energy recently reported by JYFLTRAP as 58.6(82) keV [9], improving the uncertainty from the ENSDF value of 50(50) keV [37] based on Q_{β^-} measurements [44]. This state could not be resolved from the ground state in either the TITAN Penning trap or MR-TOF-MS measurements. As in the cases of ^{125}In and ^{126}In , the reported MR-TOF-MS value for the ground-state mass of ^{130}In has been adjusted to account for the unknown ratio of ground state and isomer present. It is worth noting that this procedure was not done for the listed TITAN Penning trap mass value, which lies between the JYFLTRAP ground-state and first isomer masses. The AME2016 [3] ground-state mass for ^{130}In comes from an evaluation of Q_{β^-} measurements [44,45]. It was also measured by CPT [5], though the CPT measurement deviates by ≈ 200 keV from the other measurements and likely includes a mixture of the higher-lying isomer $^{130}\text{In}^{m2}$. The TITAN MR-TOF-MS measurement reported here agrees with the JYFLTRAP, TITAN Penning trap, and AME2016 values.

The excitation energy of $^{130}\text{In}^{m2}$ is reported in ENSDF [37] as 400(60) keV based on Q_{β^-} measurements [44]. The TITAN Penning trap measured a 41-keV shift from the ENSDF value, reporting an excitation energy of 359(34) keV. The new JYFLTRAP measurement [9], which fully resolved the ^{130}In ground state and both isomers, found a 385.5(50)-keV excitation energy for $^{130}\text{In}^{m2}$, between the TITAN Penning trap and ENSDF values. The TITAN MR-TOF-MS measured the $^{130}\text{In}^{m2}$ excitation energy to be 370(25) keV, in agreement with both Penning trap measurements.

G. ^{131}In

The ground-state mass of ^{131}In was previously measured by both JYFLTRAP [4] and CPT [5]. The CPT measurement included an unknown mixture of the ground and isomeric states and deviated from the JYFLTRAP ground-state mass by 149 keV. The TITAN MR-TOF-MS ground-state ^{131}In mass excess of $-68\,051(40)$ keV agrees with the JYFLTRAP value of $-68\,025.0(26)$ keV within the uncertainty, deviating by 26 keV in the opposite direction of the CPT deviation.

JYFLTRAP has also measured the excitation energy of the isomeric state $^{131}\text{In}^{m1}$ to be 365(8) keV [43], 63 keV higher than the previous literature value of 302(32) keV [46]. The $^{131}\text{In}^{m1}$ excitation energy measured by the TITAN MR-TOF-MS is 375(18) keV, which agrees with the JYFLTRAP value.

The $^{131}\text{In}^{m2}$ excitation energy was not previously determined by any direct mass measurements, and is listed as 3764(88) keV in ENSDF [34,37] based on Q_{β^-} measurements [46]. The TITAN MR-TOF-MS measurement of 3771(15) keV is in excellent agreement with the Q_{β^-} value and reduces the uncertainty by more than a factor of 5.

H. ^{132}In

The ground-state mass of ^{132}In was measured directly for the first time. As discussed in Sec. I, previous Penning trap mass measurements in this region have found large systematic deviations from indirect masses derived from β decay, making direct mass measurements vitally important. The AME2016 value of $-62\,410(60)$ keV for the mass excess of ^{132}In was determined via β decay [47], and agrees with the direct TITAN MR-TOF-MS mass excess of $-62\,395(38)$ keV. ^{132}In currently has no known isomeric states, and none were observed in this work.

I. ^{133}In

Prior to this work, the ground-state mass of ^{133}In had never been measured experimentally. The newly measured mass excess of $-57\,678(41)$ keV deviates from the AME2016 extrapolation by 218 keV, which is the largest deviation from the AME2016 found in this work.

This experiment also marks the first direct measurement of $^{133}\text{In}^m$, which was previously predicted based on the population of ^{133}Sn levels in ^{133}In β^- and ^{134}In β^-n decays [48]. A recent study of ^{133}Sn structure populated by ^{133}In β^- decay employed isomer-selective laser ionization of the $(9/2^+)$ ground state and the $(1/2^-)$ isomer [49], further supporting the presence of this isomer. The 642(60)-keV excitation energy measured by the TITAN MR-TOF-MS is 312 keV larger than the previously predicted value. Odd- A indium isotopes all have $9/2^+$ ground states from the $\pi(1g_{9/2})^{-1}$ proton hole state and $1/2^-$ isomers from the $\pi(2p_{1/2})^{-1}$ proton hole state. Thus the excitation energy of the $1/2^-$ isomer reflects the energy gap between the $\pi 2p_{1/2}$ and $\pi 1g_{9/2}$ orbitals. Recent studies of these isomer excitation energies for neutron-deficient indium [50,51] have demonstrated the sensitivity of this gap to neutron occupation numbers. The JYFLTRAP measurements of ^{129}In and ^{131}In isomers [43] clarified the trend of the $1/2^-$ excitation energy up to the $N = 82$ shell closure. The ^{133}In measurement reported here is the first measurement of the $1/2^-$ excitation energy beyond $N = 82$ and demonstrates a significantly larger energy gap between the $\pi 2p_{1/2}$ and $\pi 1g_{9/2}$ orbitals than previously predicted as neutrons begin filling in the new shell. This presents strong motivation for additional theoretical studies similar to those presented in Ref. [50] extending beyond $N = 82$ to pinpoint the microscopic interactions driving the increased isomer excitation energy. The trend of the $1/2^-$ excitation energy across the indium isotopic chain is presented in Fig. 4.

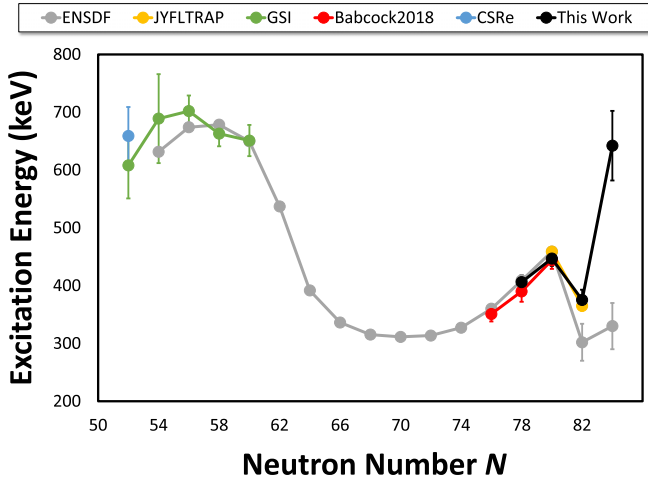


FIG. 4. Systematics of the $1/2^-$ isomer excitation energy for even- N indium isotopes, all of which have $9/2^+$ ground states. Data are taken from ENSDF [37] and recent precision mass measurements [8,43,50,51].

J. ^{134}In

The ground-state mass of ^{134}In was also measured for the first time in this work, with a mass excess of $-51\,855(44)$ keV. ^{134}In has only one known isomeric state, recently discovered with a half-life of $3.5(4)$ μs [52], which is too short lived to have been observed in the TITAN MR-TOF-MS.

V. DISCUSSION

As noted in Ref. [2], only a handful of the masses used for r -process calculations has been measured. Such calculations therefore rely heavily on mass models to predict masses far from stability. Thus the neutron-rich indium masses presented in this work are useful not only as direct inputs for r -process calculations but also as benchmarks for theoretical models, which diverge in the very neutron-rich regions where no data are available (see, for example, Fig. 6 in Ref. [2]). Figure 5 compares the TITAN data from this work and from the earlier TITAN Penning trap measurements [8] to five different mass models: Dufflo-Zuker (DZ95) [53], Hartree-Fock-Bogoliubov (HFB-24) [54], Weizsäcker-Skyrme (WS4) [55], Kura-Tachibana-Uno-Yamada (KTUY05) [56], and the finite-range droplet model (FRDM2012) [57]. Masses are plotted relative to the AME2016 values. A review of the various approaches to nuclear mass models can be found in Ref. [58]. As seen in Fig. 5, current mass models all underpredict the mass excess of $^{132-134}\text{In}$. For indium isotopes in the $N = 84-87$ range, the WS4, KTUY05, and DZ95 mass values are all in good agreement with each other, while the HFB-24 model predicts smaller masses and the FRDM2012 predicts larger masses. The FRDM2012 comes closest to the newly measured $^{132-134}\text{In}$ masses, however it still underpredicts the masses, most significantly the mass of ^{133}In by 542 keV.

The precise effect of these mass measurements on r -process abundances will not be known until they are incorporated into new network calculations for r -process nucleosynthesis and run for different astrophysical scenarios. The masses of $^{133,134}\text{In}$ were measured for the first time,

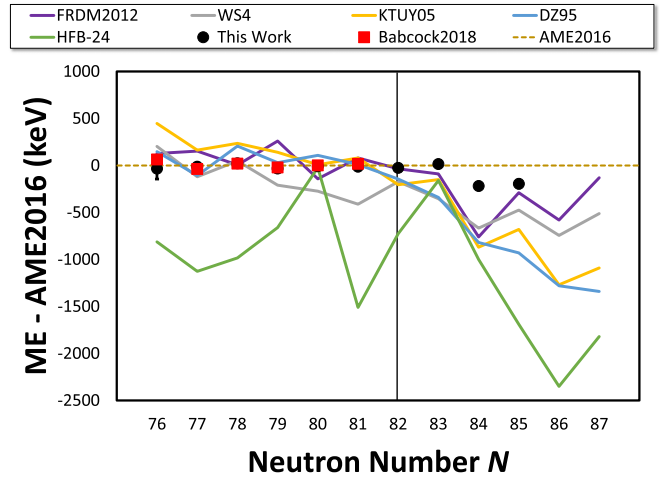


FIG. 5. Comparison of neutron-rich indium TITAN MR-TOF-MS mass measurements from this work and the previous TITAN Penning trap measurements (Babcock2018) [8] to predictions from theoretical mass models [53–57]. All masses are plotted relative to the AME2016 values [3], which include extrapolations for $N \geq 84$. The solid vertical line indicates the major shell closure at $N = 82$.

and the ^{132}In mass was measured directly for the first time, providing the first accurate mass data for $N > 82$ in the neutron-rich indium chain. As discussed in Sec. I, sensitivity studies have demonstrated that these isotopes are especially important for network calculations to accurately model the expected r -process abundances [2]. These measurements can now also be used for tuning the parameters of mass models, which deviate significantly for very neutron-rich nuclei where mass data are still unavailable. By improving the reliability of mass models, the effect of these new mass measurements may reach well beyond the direct impact of their individual masses in r -process calculations.

Furthermore, the abundance of isomers in neutron-rich indium should be accounted for in r -process calculations. In scenarios with sufficiently high temperatures, isomeric states can be thermally populated and thus the astrophysical lifetime of a given isotope may be altered from scenarios involving only decays from the ground state [59–61], especially when the half-lives of isomeric states are of the same order as (or even larger than) the respective ground-state half-lives, as is the case for the indium chain. Isomeric states may also be fed by neutron capture [60]. The survey of isomeric states presented here, particularly the cases where isomers were observed directly for the first time, may therefore be of great importance for future r -process calculations seeking to properly account for the effect of isomers.

VI. SUMMARY

The masses of neutron-rich indium isotopes from $N = 76$ to 85 were measured directly with the TITAN MR-TOF-MS, marking the first mass measurement of $^{133,134}\text{In}$ and the first direct mass measurement of ^{132}In . The uncertainties of several neutron-rich indium ground-state masses and isomer excitation energies have been improved compared to previous

literature values. These measurements provide valuable input for future r -process calculations and tests of mass models in the neutron-rich region of the $N = 82$, $Z = 50$ double shell closure.

ACKNOWLEDGMENTS

We wish to thank the TRIUMF Beam Delivery and Resonant Ionization Laser Ion Source groups for their support leading up to and during this experiment. This

work was supported by the Natural Sciences and Engineering Research Council of Canada; the National Research Council of Canada via TRIUMF; the Canada-UK Foundation; the US Department of Energy, Office of Science, under Grant No. DE-SC0017649; the BMBF (Grants No. 05P16RGFN1 and No. 05P19RGFN8), the HMWK through the LOEWE Center HICforFAIR; and the JLU and GSI under the JLU-GSI strategic Helmholtz partnership agreement.

-
- [1] E. M. Burbidge, G. R. Burbidge, W. A. Fowler, and F. Hoyle, *Rev. Mod. Phys.* **29**, 547 (1957).
- [2] M. Mumpower, R. Surman, G. McLaughlin, and A. Aprahamian, *Prog. Part. Nucl. Phys.* **86**, 86 (2016).
- [3] M. Wang, G. Audi, F. G. Kondev, W. Huang, S. Naimi, and X. Xu, *Chin. Phys. C* **41**, 030003 (2017).
- [4] J. Hakala, J. Dobaczewski, D. Gorelov, T. Eronen, A. Jokinen, A. Kankainen, V. S. Kolhinen, M. Kortelainen, I. D. Moore, H. Penttilä *et al.*, *Phys. Rev. Lett.* **109**, 032501 (2012).
- [5] J. Van Schelt, D. Lascar, G. Savard, J. A. Clark, P. F. Bertone, S. Caldwell, A. Chaudhuri, A. F. Levand, G. Li, G. E. Morgan *et al.*, *Phys. Rev. Lett.* **111**, 061102 (2013).
- [6] J. Van Schelt, D. Lascar, G. Savard, J. A. Clark, S. Caldwell, A. Chaudhuri, J. Fallis, J. P. Greene, A. F. Levand, G. Li *et al.*, *Phys. Rev. C* **85**, 045805 (2012).
- [7] J. Dilling, R. Baartman, P. Bricault, M. Brodeur, L. Blomeley, F. Buchinger, J. Crawford, J. R. Crespo López-Urrutia, P. Delheij, M. Froese *et al.*, *Int. J. Mass Spectrom.* **251**, 198 (2006).
- [8] C. Babcock, R. Klawitter, E. Leistenschneider, D. Lascar, B. R. Barquest, A. Finlay, M. Foster, A. T. Gallant, P. Hunt, B. Kootte *et al.*, *Phys. Rev. C* **97**, 024312 (2018).
- [9] D. A. Nesterenko, A. Kankainen, J. Kostensalo, C. R. Nobs, A. M. Bruce, O. Beliuskina, L. Canete, T. Eronen, E. R. Gamba, S. Geldhof *et al.*, *Phys. Lett.* **808**, 135642 (2020).
- [10] C. Jesch, T. Dickel, W. R. Plaß, D. Short, S. Ayet San Andres, J. Dilling, H. Geissel, F. Greiner, J. Lang, K. G. Leach *et al.*, *Hyperfine Interactions* **235**, 97 (2015).
- [11] T. Dickel, S. A. San Andrés, S. Beck, J. Bergmann, J. Dilling, F. Greiner, C. Hornung, A. Jacobs, G. Kripko-Koncz, A. Kwiatkowski *et al.*, *Hyperfine Interactions* **240**, 62 (2019).
- [12] G. C. Ball, G. Hackman, and R. Krücken, *Physica Scripta* **91**, 093002 (2016).
- [13] S. Raeder, H. Heggen, J. Lassen, F. Ames, D. Bishop, P. Bricault, P. Kunz, A. Mjøs, and A. Teigelhöfer, *Rev. Sci. Instrum.* **85**, 033309 (2014).
- [14] P. Bricault, R. Baartman, M. Domsby, A. Hurst, C. Mark, G. Stanford, and P. Schmor, *Nucl. Phys.* **701**, 49 (2002).
- [15] T. Brunner, M. Smith, M. Brodeur, S. Ettenauer, A. Gallant, V. Simon, A. Chaudhuri, A. Lapiere, E. Mané, R. Ringle *et al.*, *Nucl. Inst. Methods Phys. Res. Sec. A* **676**, 32 (2012).
- [16] W. R. Plaß, T. Dickel, U. Czok, H. Geissel, M. Petrick, K. Reinheimer, C. Scheidenberger, and M. I. Yavor, *Nucl. Inst. Methods Phys. Res. Sec. B* **266**, 4560 (2008).
- [17] T. Dickel, W. Plaß, A. Becker, U. Czok, H. Geissel, E. Haettner, C. Jesch, W. Kinsel, M. Petrick, C. Scheidenberger *et al.*, *Nucl. Inst. Methods Phys. Res. Sec. A* **777**, 172 (2015).
- [18] A. E. Cameron and D. F. Eggers, *Rev. Sci. Instrum.* **19**, 605 (1948).
- [19] W. C. Wiley and I. H. McLaren, *Rev. Sci. Instrum.* **26**, 1150 (1955).
- [20] M. I. Yavor, W. R. Plaß, T. Dickel, H. Geissel, and C. Scheidenberger, *Int. J. Mass Spectrom.* **381-382**, 1 (2015).
- [21] C. Will, B.S. thesis, University of Giessen, 2017.
- [22] T. Dickel, M. I. Yavor, J. Lang, W. R. Plaß, W. Lippert, H. Geissel, and C. Scheidenberger, *Int. J. Mass Spectrom.* **412**, 1 (2017).
- [23] T. Dickel, W. R. Plaß, W. Lippert, J. Lang, M. I. Yavor, H. Geissel, and C. Scheidenberger, *J. American Soc. Mass Spectrometry* **28**, 1079 (2017).
- [24] S. Beck, B. Kootte, I. Dedes, T. Dickel, A. Kwiatkowski, M. Lykiardopoulou, W. R. Plaß, M. P. Reiter, J. Bergmann, D. Curien *et al.* (unpublished).
- [25] J. Ebert, Ph.D. thesis, Justus-Liebig-Universität Giessen, 2016.
- [26] S. Ayet San Andrés, C. Hornung, J. Ebert, W. R. Plaß, T. Dickel, H. Geissel, C. Scheidenberger, J. Bergmann, F. Greiner, E. Haettner *et al.*, *Phys. Rev. C* **99**, 064313 (2019).
- [27] S. Purushothaman, S. A. S. Andrés, J. Bergmann, T. Dickel, J. Ebert, H. Geissel, C. Hornung, W. Plaß, C. Rappold, C. Scheidenberger *et al.*, *Int. J. Mass Spectrom.* **421**, 245 (2017).
- [28] G. Audi, F. G. Kondev, M. Wang, W. Huang, and S. Naimi, *Chin. Phys. C* **41**, 030001 (2017).
- [29] J. Katakura, *Nucl. Data Sheets* **114**, 1497 (2013).
- [30] J. Katakura and K. Kitao, *Nucl. Data Sheets* **97**, 765 (2002).
- [31] A. Hashizume, *Nucl. Data Sheets* **112**, 1647 (2011).
- [32] Z. Elekes and J. Timar, *Nucl. Data Sheets* **129**, 191 (2015).
- [33] J. Timar, Z. Elekes, and B. Singh, *Nucl. Data Sheets* **121**, 143 (2014).
- [34] Y. Khazov, I. Mitropolsky, and A. Rodionov, *Nucl. Data Sheets* **107**, 2715 (2006).
- [35] Y. Khazov, A. Rodionov, and F. Kondev, *Nucl. Data Sheets* **112**, 855 (2011).
- [36] A. Sonzogni, *Nucl. Data Sheets* **103**, 1 (2004).
- [37] From ENSDF database as of January 14, 2020. Version available at <http://www.nndc.bnl.gov/ensarchivals/>
- [38] P. Hoff, B. Ekström, H. Göktürk, and B. Fogelberg, *Nucl. Phys.* **459**, 35 (1986).
- [39] H. Huck, A. Jech, G. Martí, M. L. Pérez, J. J. Rossi, and H. M. Sofía, *Phys. Rev. C* **39**, 997 (1989).
- [40] B. Fogelberg, H. Mach, H. Gausemel, J. Omtvedt, and K. Mezilev, *AIP Conf. Proc.* **447**, 191 (1998).
- [41] O. Arndt, S. Hennrich, N. Hotelling, C. Jost, B. Tomlin, J. Shergur, K.-L. Kratz, P. Mantica, B. Brown, R. Janssens *et al.*, *Acta Phys. Pol. B* **40**, 437 (2009).

- [42] H. Gausemel, B. Fogelberg, T. Engeland, M. Hjorth-Jensen, P. Hoff, H. Mach, K. A. Mezilev, and J. P. Omtvedt, *Phys. Rev. C* **69**, 054307 (2004).
- [43] A. Kankainen, J. Hakala, T. Eronen, D. Gorelov, A. Jokinen, V. S. Kolhinen, I. D. Moore, H. Penttilä, S. Rinta-Antila, J. Rissanen *et al.*, *Phys. Rev. C* **87**, 024307 (2013).
- [44] L. Spanier, K. Aleklett, B. Ekström, and B. Fogelberg, *Nucl. Phys.* **474**, 359 (1987).
- [45] U. Stöhlker, A. Blönnigen, W. Lippert, and H. Wollnik, *Z. Phys. A* **336**, 369 (1990).
- [46] B. Fogelberg, H. Gausemel, K. A. Mezilev, P. Hoff, H. Mach, M. Sanchez-Vega, A. Lindroth, E. Ramström, J. Genevey, J. A. Pinston *et al.*, *Phys. Rev. C* **70**, 034312 (2004).
- [47] K. A. Mezilev, Y. N. Novikov, A. V. Popov, B. Fogelberg, and L. Spanier, *Physica Scripta* **T56**, 272 (1995).
- [48] P. Hoff, P. Baumann, A. Huck, A. Knipper, G. Walter, G. Marguier, B. Fogelberg, A. Lindroth, H. Mach, M. Sanchez-Vega *et al.* (ISOLDE Collaboration), *Phys. Rev. Lett.* **77**, 1020 (1996).
- [49] M. Piersa, A. Korgul, L. M. Fraile, J. Benito, E. Adamska, A. N. Andreyev, R. Álvarez-Rodríguez, A. E. Barzakh, G. Benzoni, T. Berry *et al.* (IDS Collaboration), *Phys. Rev. C* **99**, 024304 (2019).
- [50] X. Xu, J. H. Liu, C. X. Yuan, Y. M. Xing, M. Wang, Y. H. Zhang, X. H. Zhou, Y. A. Litvinov, K. Blaum, R. J. Chen *et al.*, *Phys. Rev. C* **100**, 051303(R) (2019).
- [51] C. Hornung, D. Amanbayev, I. Dedes, G. Kripko-Koncz, I. Miskun, N. Shimizu, S. Ayet San Andrés, J. Bergmann, T. Dickel, J. Dudek *et al.*, *Phys. Lett.* **802**, 135200 (2020).
- [52] V. H. Phong, G. Lorusso, T. Davinson, A. Estrade, O. Hall, J. Liu, K. Matsui, F. Montes, S. Nishimura, A. Boso *et al.*, *Phys. Rev. C* **100**, 011302 (2019).
- [53] J. Duflo and A. P. Zuker, *Phys. Rev. C* **52**, R23 (1995).
- [54] S. Goriely, N. Chamel, and J. M. Pearson, *Phys. Rev. C* **88**, 024308 (2013).
- [55] N. Wang, M. Liu, X. Wu, and J. Meng, *Phys. Lett. B* **734**, 215 (2014).
- [56] H. Koura, T. Tachibana, M. Uno, and M. Yamada, *Prog. Theor. Phys.* **113**, 305 (2005).
- [57] P. Möller, A. Sierk, T. Ichikawa, and H. Sagawa, *At. Data Nucl. Data Tables* **109-110**, 1 (2016).
- [58] D. Lunney, J. M. Pearson, and C. Thibault, *Rev. Mod. Phys.* **75**, 1021 (2003).
- [59] M. Arnould, S. Goriely, and K. Takahashi, *Phys. Rep.* **450**, 97 (2007).
- [60] G. Martínez-Pinedo and K. Langanke, *Phys. Rev. Lett.* **83**, 4502 (1999).
- [61] R. Reifarth, S. Fiebiger, K. Göbel, T. Heftrich, T. Kausch, C. Köppchen, D. Kurtulgil, C. Langer, B. Thomas, and M. Weigand, *Int. J. Mod. Phys. A* **33**, 1843011 (2018).